A simple generalized mass transfer model for evaluation of the environmental performance of archival boxes

Check for updates

Jernej Markelj[1], Josep Grau-Bove[2], Ida Kraševec[1], Evy Vereecken[3,4] & Matija Strlič[1,2,5] ✉

Enclosure materials can have a variety of properties that moderate relative humidity (RH) in relation to external RH fluctuations. In this study of different constructions and board types we developed a simple empirical model to predict the relative humidity damping capacity via a Humidity Attenuation (HA) index. A multiple linear regression model was built to predict the HA index based on the material/box properties. The results indicate that at low ventilation rates, vapour permeability has a similar (but opposite) effect to moisture buffering and that stacking boxes or filling them with paper significantly improves the enclosure's RH damping capacity. This work will provide a more realistic assessment of the suitability of museum enclosure microenvironments with respect to RH moderation. To increase applicability in practice, a decision-making tool (an online app) was developed for curators and conservators to support preventive conservation measures.

In collection storage, boxes and other enclosures, from wrappings to crates, are used to enable safe handling, but also to protect objects from dust, pests and humidity fluctuations, to protect against rapid spread of fire, or to protect objects that are too fragile for individual handling (see Fig. 1)[1]. Although such enclosures are mostly meant as physical protection, a proper choice of the enclosure material can significantly affect the internal microenvironment and thus offers additional preventive conservation benefits[2,3].

Hygroscopic enclosure materials can "buffer" moisture. In the context of moisture and enclosures, "buffering" refers to the capacity of materials or systems to absorb and release moisture when exposed to respectively high and low relative humidity (RH) within the enclosure, and in this way to moderate fluctuations in RH within an indoor environment[4–7]. Moisture buffering helps to stabilize indoor conditions, by reducing the amplitude and speed of humidity variations caused by external changes or indoor activities such as cooking, bathing, or ventilation. In conservation, buffering is a desirable property of enclosures, from storage boxes to display cases, because lower fluctuations mean a lower risk of mechanical damage. In addition to moisture buffering, also other aspects, such as for instance the air change rate, can have an impact on the moderation of the relative humidity within enclosures. In the current study, we use the term "RH damping capacity" when it comes to reducing the amplitude in relative humidity because of the full combination of enclosure properties, including the design. Because of lower RH fluctuations have a positive effect on the

preventive conservation of collections, there is an interest in understanding which enclosure properties lead to a good RH damping capacity[8–11].

In Part I of this series, we looked at some typical methods used to assess the environmental impact of the enclosure material on the microenvironment within, specifically focusing on humidity[12]. Although the explored enclosures' materials offer some thermal barrier properties, these are minimal, and the paper focused on the assessment of properties that affect water transport: (i) air exchange rate was determined using the CO_2 dissipation method; (ii) water vapour transport rate was determined using the gravimetric method according to the ISO 2528:2017 standard; (iii) moisture sorption isotherms was determined using the gravimetric method. Additionally, in Part I, we explored the environmental behaviour of 25 different enclosures made of diverse cardboard and paper, as well as moisture barrier and textile materials, and different designs (clamshell, 2-part, with holes and without, sealed and not). Also, both enclosures filled with paper or not, and exposed to RH fluctuations either separated or stacked, were analysed. This all resulted in a significant collection of RH data, examples of which are presented therein[12].

In the current study (Part II), we explore whether this data can be used to develop a generalised model of enclosure behaviour with respect to humidity, using a simple mass transfer model. The model developed here could help curators and conservators to select suitable enclosure materials for storage environments experiencing specific humidity variations. It is clear that enclosure materials can effectively prevent even significant humidity

[1]Heritage Science Laboratory Ljubljana, Faculty of Chemistry and Chemical Technology, University of Ljubljana, Ljubljana, Slovenia. [2]Institute for Sustainable Heritage, University College London, London, UK. [3]Building Physics and Sustainable Design, Department of Civil Engineering, KU Leuven, Leuven, Belgium. [4]Monuments and Monumental Decoration Lab, Royal Institute for Cultural Heritage (KIK-IRPA), Brussels, Belgium. [5]Museum Conservation Institute, Smithsonian Institution, Suitland, MD, USA. ✉e-mail: Matija.Strlic@fkkt.uni-lj.si

Fig. 1 | Example of enclosures. Enclosures, from wrappings to boxes and crates, offer different conservation benefits to objects stored within, including mechanical and environmental protection.

variations, however, they cannot protect from consistently high relative humidity or condensation caused by large and sudden temperature drops. The paper also puts forward a set of parameters that can be used to describe the humidity damping properties of an enclosure. The model is also available in the form of an online app (https://hsll.shinyapps.io/ha_index_pub/).

Section 2 first gives an overview of the studied archival boxes and describes the techniques applied for measuring temperature and relative humidity as well as the simple one-parameter model and the statistical methods applied in the study. For reasons of completeness also an overview of the measurement techniques used to characterize the enclosure's properties will be reiterated and the measured properties are summarized. Next, in section 3 we present the results achieved based on the simple one-parameter model and how this RH damping capacity could be predicted based on box properties. In the last section we discuss a comparison with other moisture models, the evaluation of boxes' sustainability in terms of their RH damping capacity, and the online app for assessing the suitability of storage boxes.

The role of enclosures in the accumulation of gases emitted by heritage materials themselves is often discussed, specifically in relation to acetic acid, a prevalent indoor-generated pollutant in collections[13]. This is often of concern for objects made of cellulose acetate and a model has recently been proposed to describe its accumulation in boxes depending on the emission rates from objects[14,15]. Conversely, it is well known that while material-generated volatiles accumulate in enclosures, these also protect the stored material from externally generated pollutants[16]. Since acetic acid, as the most prevalent organic volatile acid found in collection storage is not thought to be a concern to the degradation of cellulosic materials[17] and a manageable threshold of 100 ppb has been proposed for long-term storage (PAS 198:2012), this paper does not deal with pollutant retention/protection properties of storage enclosures.

Methods
Archival boxes
Forty-eight unique storage boxes from different manufacturers with different designs (2-piece box, flap box with flaps on the longer or shorter side,

single- or double-wall, wrapped, with or without holes and glue), sizes (A3, A4, and A5) and materials (JPP cardboard, textile, cardboard with textile lining, coated cardboard, corrugated cardboard, PE and PP plastic, micro-perforated plastic) were studied (see Table 1).

Within this study, boxes were divided into the following six groups according to the type of material: 1) "Cardboard" group, which consists of JPP boxes with a wall thickness of 1 mm (JPP1) and 0.65 mm (JPP.65). This group also includes JPP cardboard box impregnated with Paraloid (A4 CLAMss JPP1 Paraloid) and layered textile box made from tyvek, cotton canvas and nylon thick weave from MS (A4 Textile wrap); 2) "Cardboard-Coated/ > 1 mm group" - this group includes JPP1 boxes coated with various materials (Moistop, EVA or self-adhesive tape), JPP box with 1.3 mm wall thickness (JPP1.3), recycled storage box with 1.8 mm wall thickness from CXD and NUK boxes with very thick walls (>5.2 mm) made of cardboard, textile lining and MEKOL or LINECO glue; 3) "Cardboard-Flute" group - includes boxes made of corrugated cardboard with different fluting profiles (E, EB and FE) and designs; 4) "Plastic" group - consists of boxes made of PP and PE plastic with different design; 5) "Plastic- Micro-perforated" group - includes boxes made of PP plastic hollow-wall micro-perforated sheets with different design; 6) "Kraft" group - two boxes made of kraft paper wrapped around a simple metal construction. Kraft paper was either coated with PE (A4 Kraft wrap PE) or not (A4 Kraft wrap).

Measurements of relative humidity and temperature
The boxes were placed in a test environment where the external relative humidity (RH) was altered as would be expected from a poor storage environment (see Discussion section). The purpose of these changes was to mimic and study naturally occurring fluctuations in indoor storage spaces.

Relative humidity (RH) and temperature (T) were measured outside and inside the boxes over a period of 3 to 13.6 days, with sampling time of 5 min for all measurements, using small battery-powered loggers (Onset HOBO, Massachusetts, USA), as shown in Figure SM1[18,19]. Changes in external relative humidity (RH_e) and temperature (T_e) were promoted by humidification, dehumidification, and heating in a range between 33–80% (excluding short spikes) and 16.6–23.4 °C, respectively. Measurements were

Table 1 | List of boxes used in the study[a]

ID	Box code[b]	Group[c]	Design [d]	Material	Manufacturer	Note
1	A4 2-P GL JPP1 E[e, g]	Cardboard	2-P	JPP1	JPP	Cardboard-Glued.
2	A4 2-P GL JPP1 H E[e,g]	Cardboard	2-P	JPP1	JPP	Cardboard-Glued&Holes.
3	A4 CLAMls GL JPP1 E	Cardboard	CLAMls	JPP1	JPP	Cardboard-Glued.
4	A4 CLAMss CL JPP1 E[e,g]	Cardboard	CLAMss	JPP1	JPP	Cardboard.
5	A4 CLAMss CL JPP1 H E[e]	Cardboard	CLAMss	JPP1	JPP	Cardboard-Holes.
6	A4 2-P GL JPP1 sealed E[e,g]	Cardboard	2-P	JPP1	JPP	Cardboard-Glued&Sealed slits.
7	A4 CLAMls CL JPP.65 E[f]	Cardboard	CLAMls	JPP.65	JPP	Cardboard-0.65 mm wall thickness.
8	A3 CLAMss CL JPP1 E[f]	Cardboard	CLAMss	JPP1	JPP	Cardboard-Size A3.
9	A5 CLAMss CL JPP1 E[f]	Cardboard	CLAMss	JPP1	JPP	Cardboard-Size A5.
10	A4 CLAMss JPP1 Paraloid	Cardboard	CLAMss	JPP1 + Paraloid	JPP	Cardboard impregnated with Paraloid.
11	A4 Textile wrap	Cardboard	Wrap	MS (textile)	MS	Layered textile: tyvek + cotton canvas + Nylon thick weave.
12	A4 CLAMls GL Recy E[e]	Cardboard-Coated/ > 1 mm	CLAMls	CXD EcopHant	CXD	Recycled Archival Storage Box-Glued.
13	A4 CLAMls CL JPP1.3 E[f]	Cardboard-Coated/ > 1 mm	CLAMls	JPP1.3	JPP	Cardboard-1.3 mm wall thickness.
14	A4 CLAMss JPP1 EVA	Cardboard-Coated/ > 1 mm	CLAMss	JPP1 + EVA	JPP	Cardboard-Coated with EVA.
15	NUK mekol glue	Cardboard-Coated/ > 1 mm	CLAMls	Mekol	NUK	Cardboard with textile lining (Solander box), made with MEKOL glue.
16	NUK mekol glue (holes)	Cardboard-Coated/ > 1 mm	CLAMls	Mekol	NUK	Cardboard with textile lining (Solander box), made with MEKOL glue (holes).
17	NUK lineco glue	Cardboard-Coated/ > 1 mm	CLAMls	Lineco	NUK	Cardboard with textile lining (Solander box), made with LINECO glue.
18	NUK lineco glue (holes)	Cardboard-Coated/ > 1 mm	CLAMls	Lineco	NUK	Cardboard with textile lining (Solander box), made with LINECO glue (holes).
19	A4 2-P GL JPP1 coated E[g]	Cardboard-Coated/ > 1 mm	2-P	JPP1 + Tape	JPP	Cardboard-Glued&Coated with self adhesive tape.
20	A4 CLAMss JPP1 Moistop	Cardboard-Coated/ > 1 mm	CLAMss	JPP1 + Moistop	JPP	Cardboard-Layered with Moistop.
21	A4 CLAMls CL JPPflut E[f]	Cardboard-Flute	CLAMls	CXD Corrugated	CXD	Cardboard-Flute.
22	IKS_WP851	Cardboard-Flute	CLAMls	WP851	ZFB	Cardboard-E Flute.
23	IKS6DW_WP851	Cardboard-Flute	CLAMls dw	WP851	ZFB	Cardboard-E Flute.
24	ISS_WP851	Cardboard-Flute	2-P	WP851	ZFB	Cardboard-E Flute.
25	ISS8DW_WP851	Cardboard-Flute	2-P dw	WP851	ZFB	Cardboard-E Flute.
26	IKS_WP821	Cardboard-Flute	CLAMls	WP821	ZFB	Cardboard-EB Flute.
27	IKS6DW_WP821	Cardboard-Flute	CLAMls dw	WP821	ZFB	Cardboard-EB Flute.
28	ISS_WP821	Cardboard-Flute	2-P	WP821	ZFB	Cardboard-EB Flute.
29	ISS8DW_WP821	Cardboard-Flute	2-P dw	WP821	ZFB	Cardboard-EB Flute.
30	IKS_WP811	Cardboard-Flute	CLAMls	WP811	ZFB	Cardboard-FE Flute.
31	IKS6DW_WP811	Cardboard-Flute	CLAMls dw	WP811	ZFB	Cardboard-FE Flute.
32	ISS_WP811	Cardboard-Flute	2-P	WP811	ZFB	Cardboard-FE Flute.
33	ISS8DW_WP811	Cardboard-Flute	2-P dw	WP811	ZFB	Cardboard-FE Flute.
34	A4 Kraft wrap	Kraft	Wrap	Kraft	MS	Kraft paper.
35	A4 Kraft wrap PE	Kraft	Wrap	coated Kraft	MS	Kraft paper with a PE coating.
36	IKS_PP105	Plastic	CLAMls	PP105	ZFB	PP Plastic Hollow-wall sheet.
37	IKS6DW_PP105	Plastic	CLAMls dw	PP105	ZFB	PP Plastic Hollow-wall sheet.
38	ISS_PP105	Plastic	2-P	PP105	ZFB	PP Plastic Hollow-wall sheet.
39	ISS8DW_PP105	Plastic	2-P dw	PP105	ZFB	PP Plastic Hollow-wall sheet.
40	A4 CLAMls Prague1a	Plastic	CLAMls	Prague No. 1a	Prague	Plastic.
41	A4 2-part Prague1b	Plastic	2-P	Prague No. 1b	Prague	Plastic-Glued.
44	A4 CLAMls Prague2a	Plastic	CLAMls	Prague No. 2b	Prague	Plastic
42	A4 2-part Prague2b	Plastic	2-P	Prague No. 2b	Prague	Plastic-Glued.
43	A4 CLAMls CXDPE	Plastic	CLAMls	CXD Polyphlute	CXD	PE Plastic.

Table 1 (continued) | List of boxes used in the study[a]

ID	Box code[b]	Group[c]	Design [d]	Material	Manufacturer	Note
45	IKS_PP104	Plastic-Microperforated	CLAMls	PP104	ZFB	PP Plastic Hollow-wall sheet-Microperforated.
46	IKS6DW_PP104	Plastic-Microperforated	CLAMls dw	PP104	ZFB	PP Plastic Hollow-wall sheet-Microperforated.
47	ISS_PP104	Plastic-Microperforated	2-P	PP104	ZFB	PP Plastic Hollow-wall sheet-Microperforated.
48	ISS8DW_PP104	Plastic-Microperforated	2-P dw	PP104	ZFB	PP Plastic Hollow-wall sheet-Microperforated.

[a]Dimension for all boxes is 305 x 210 x 70 mm (A4), except for "A3 CLAMss CL JPP1 E" and "A5 CLAMss CL JPP1 E", which have the following dimensions: 420x305x70 mm and 210 x 105 x 70 mm, respectively.

[b]Box code is a unique name of a box (used herein). Box code in this table refers to measurements of T and RH fluctuations done with empty and unstacked boxes.

[c]Boxes were grouped, for the purpose of this study. Note however that "A4 Textile wrap" was put into Cardboard group because of similar properties to cardboard boxes in terms of RH damping capacity. Similarly, "A4 CLAMss JPP1 Paraloid" was also put into Cardboard group.

[d]Box design description: "2-P" – 2-part box. i.e. telescope box. "2-P dw" – 2-part box. i.e. telescope box. double walled. "CLAMls" – flap box with flaps on the longer side. "CLAMls dw" – flap box with flaps on the longer side. double walled. "CLAMss" – flap box with flaps on the shorter side. "Wrap" – material (Kraft/Kraft PE paper or Textile) is wrapped around simple metal construction.

[e]Measurements of T and RH fluctuations with empty and unstacked boxes were done in replicates (uncertainty assessment).

[f]Boxes used in measurements of T and RH fluctuations – filled with stack of paper. Box codes: A3 CLAMss CL JPP1 F, A4 CLAMls CL JPP.65 F, A4 CLAMls CL JPP1.3 F, A4 CLAMls CL JPPflut F, A5 CLAMss CL JPP1 F.

[g]Boxes used in a "stack" experiment (for T and RH fluctuations measurements). Box codes: A4 2-P GL JPP1 STACK, A4 2-P GL JPP1 H STACK, A4 2-P GL JPP1 sealed STACK, A4 2-P GL JPP1 coated STACK, A4 CLAMss CL JPP1 STACK.

performed in nine experimental runs, with multiple boxes placed in the same test environment (Figure SM2). The measurement periods and ranges of measured data (RH_e and T_e) for each series of experiments are listed in Table SM1. A low air velocity was maintained for all measurements (approximately 0.02 m/s). An example of the measurements of RH and T for carboard box "A4 2-P GL JPP1 sealed E" and corrugated cardboard box "IKS_WP821" is shown in Figure SM3.

While the loggers from Onset HOBO have an accuracy of ±2.5% for RH, most of the in-out differences evaluated in the experiments exceed this value. The accuracy of T for these loggers was ±0.2 °C.

The boxes were used in three types of experiments. First, measurements were made with empty boxes in which the entire surface of the box was exposed to external conditions by maintaining a distance of approximately 14 cm between boxes. This type of measurement was performed for all 48 boxes, with replicates for six boxes (to evaluate uncertainty). In addition, measurements were made by either filling the boxes with printing paper (five boxes) or by stacking the boxes on top of each other and thus restricting most of the surface area to the direct external conditions, leaving only the side surfaces exposed (five boxes). Figure SM2 shows the measurements with empty boxes in the "unstack" and "stack" experiments.

All data on measurements of RH and T is available from the corresponding author on reasonable request.

Description of the one-parameter model
Within the current study, the goal was to build an as simple model as possible which would adequately describe attenuation of RH inside the box when exposed to external RH fluctuations. A simple model based on relative humidity is chosen:

$$\frac{dRH_a}{dt} = s \cdot \left(RH_e - RH_a \right),$$ (1)

where RH_e (%) and RH_a (%) are relative humidity outside and inside the box, respectively, and s a fitting parameter that describes the enclosure's damping capacity. The parameter s needs to be calculated for each box.

This equation can be solved as a first order difference equation (Euler method) where the new value of $\widehat{RH}_a$ is calculated using the previous values of $\widehat{RH}_a$ as:

$$\text{initial condition}: \widehat{RH}_a(t=0) = RH_a(t=0),$$ (2)

$$\widehat{RH}_a(t+1) = s \cdot \left(RH_e(t+1) - \widehat{RH}_a(t) \right) \cdot dt + \widehat{RH}_a(t).$$ (3)

Parameter s was obtained for each experiment for each box by minimizing the residual sum of squares between the modeled and experimentally

determined relative humidity inside the box:

$$\text{RSS} = \sum_{t=1}^{N} \left(RH_a - \widehat{RH}_a \right)^2,$$ (4)

by using modification of the Levenberg Marquardt algorithm.

Root Mean Square Error (RMSE) was used for the evaluation of the model. The RMSE minimizes the sum square of the difference between the modeled and experimentally determined relative humidity inside the box:

$$\text{RMSE} = \sqrt{\left(\frac{1}{N} \cdot \sum_{t=1}^{N} \left(RH_a - \widehat{RH}_a \right)^2 \right)},$$ (5)

where N is the number of data points. RMSE has the same units as the data and gives information on the average deviation from the actual data.

All data analysis and modeling were performed using the statistical computer software language R[20]. Main R packages used in this study are listed in the Supplementary Materials.

A modified version of this model was also tested, where RH was replaced by the vapour pressure in all the equations:

$$\frac{dp_a}{dt} = s_p \cdot \left(p_e - p_a \right),$$ (6)

where p_e and p_a are the vapour pressure outside and inside the box (Pa), respectively, and s_p a fitting parameter that describes the enclosure's damping capacity (when used in the vapour pressure model) (units: -).

In addition, the effective capacitance model, written based on the Hygrothermal Inertia of the Room or storage enclosure (HIR)[21], used for comparison as described in the literature[22]

$$\left(\frac{V}{R_V T_a} + \frac{100 \cdot \text{HIR}^* \cdot V}{p_{v,sat}(T_a)} \right) \cdot \frac{\partial p_{va}}{\partial t} = \left(p_e - p_a \right) \cdot \frac{nV}{3600 \cdot R_V \cdot T_a} + G_{vp},$$ (7)

where p_e and p_a are the vapour pressure outside and inside the box (Pa), T_e and T_a are the temperature outside and inside the box (K), V is the volume of the storage enclosure (m³), n (h⁻¹) the air exchange rate, G_{vp} the vapour production in the enclosure which can be omitted in our study (kg/m³), R_v is the gas constant for water vapour (462 J/kg.K), t is the time (s) and HIR* (kg/m³.%RH) the (production-adaptive) hygric inertia per cubic meter of a room (or storage enclosure in this case)[21]. This model presumes that the humidity in the active part of the enclosure's wall is always in equilibrium with the air humidity within the storage box. The HIR*-value can be linked

to the (production-adaptive) moisture buffer value (MBV) of the enclosure's walls via:

$$\text{HIR}^* = \frac{\sum\left(A_k \cdot \text{MBV}_k^*\right) + \sum\left(\text{MBV}_l'^*\right)}{V} \qquad (8)$$

where A_k the area in contact with the indoor environment in the storage enclosure (m²), MBV^*_k the moisture buffer value of surface k (kg/(m².%RH)), MBV'^*_l the moisture buffer value of an object such as a bunch of papers in the storage enclosure (kg/%RH) and V the volume of the storage enclosure (m³).

Measurements of various material/box properties

The following physical properties were measured for each material/box: water vapour transmission rates (WVTR), moisture sorption isotherms (MSI) and air-exchange rates (AER).

The water vapour transmission rate (WVTR) is the mass of water vapour that passes through a specific area of the tested porous material in the predetermined time, at a steady state and under a specified vapour pressure difference (typical unit g/(m² day)). The WVTR for box materials was determined with a gravimetric method, according to an ISO 2528:2017 standard for sheet materials[23]. Samples were cut into circles and placed in a climate chamber for at least a day, so the materials were pre-conditioned to the test environment (30 °C, 50% RH). The edges of corrugated materials were closed with adhesive tape. Then, the desiccant $CaCl_2$ was placed on the bottom of the testing dishes, covered with the test material and an aluminium ring. The edges of the samples were carefully sealed with molten wax. After solidifying, the wax seal was inspected for cracks and holes and repaired if necessary. Then, the dishes were transported into the climate chamber (Fig. SM4) with fixed T and RH (30 °C, 50%) and weighted in regular intervals on an analytical scale. The weighting intervals were at least 1 h, the desired mass uptake between measurements being at least 0.05 g. The weighting was continued until at least four consecutive measurements with differences in mass uptake less than 5% were obtained. The WVTR was calculated as: WVTR = Δm / ($\Delta t\, S$), where Δm is the mass increase per time interval Δt, and S is the area, set to 0.0050 m². Each material was measured in two repetitions and the average WVTR was calculated (Fig. SM5). The data is collected in Table SM2. WVTR is given in g/(m²day) and the relative difference between two repetitions is listed. The limit of determination was determined to be 1 g/(m²day), which is in agreement with the standard used.

Moisture sorption isotherms (MSI) describe the moisture content in a material at different RH at constant T. Therefore, these isotherms describe the moisture storage in case of absorption and desorption, which may differ from each other and have to be measured in separate experiments[24]. The measurements were performed in a glove box, which was used to ensure stable conditions. The glove box was placed inside a thermostated room (T controlled by room air conditioning system to 18 ± 0.5 °C). The humidity was set using mixtures of water and glycerol at different ratios and the conditions were followed using an Onset HOBO T and RH logger. The air inside the glove box was homogenised through the use of two fans. The box materials were cut into 1.5 × 1.5 cm pieces (in 2-3 repetitions) and placed into the glove box together with a microanalytical balance (Fig. SM6). After the RH was set using the glycerol mixtures, selected box material samples were weighted once per day until their mass stabilized. Then, all samples were weighted, and the RH level was changed in order to measure a next point of the moisture sorption isotherm. During weighting, the fans were turned off to reduce the balance instability. RH values were increased from 11 to 78% and were then reduced back to 18%. Finally, the material samples were dried at 105 °C overnight and the dry weight was measured at the same balance. In this way, the equilibrium moisture content of a material at any RH can be calculated from the data, collected in Table SM3. An example of MSI plot for box material JPP1 is shown in Fig. SM7. The slopes of the MSI were calculated at four RH levels: 10.93%, 23.88%, 41.99% and 58.40%. Table SM4 summarizes the results, i.e., MSI slopes together with R² and

slope error based on repetitions. The limit of determination was determined to be 0.002, based on the experimental data. Experimental uncertainty is between 1.0 and 3.4% with median of 1.5%.

The air exchange rate (AER) defines the amount of times the air inside a box exchanges with the outside air in one hour both through material walls and through the holes and cracks in the box construction. It is determined by filling the box with CO_2 and measuring the reduction of its concentration as it escapes from the box. The procedure is described by Novak et al.[12]. The measured box was removed from any other surfaces; the bottom wall was raised from the table (Figure SM8). CO_2 from a can was injected into the box through a small hole until the sensor capacity was exceeded (over 5000 ppm). The hole was closed, and the reduction of CO_2 concentration measured. The average air velocity outside the boxes was 0.02 m/s. The temperature and relative humidity in the room were stable during the experiment (20 ± 2 °C, 50–60% RH). The values are collected in Table SM5.

Description of the multiple linear regression model using material/box properties

Parameter s was predicted from material/box properties using the following multiple linear regression (MLR) model:

$$s = \beta_0 + \beta_1 \frac{\text{AER}}{\text{MSI}} + \beta_2 \frac{\text{WVTR}}{\text{MSD}}. \qquad (9)$$

The "Material Surface Density" (MSD) was calculated by dividing the mass of the "active material" by the outer surface area of the boxes

$$\text{MSD} = \frac{\text{mass of "active" material [g]}}{\text{outer surface area of the box [m}^2]} \qquad (10)$$

For non-plastic boxes it was assumed that the whole material is actively participating in thermo-hygrometric processes, hence, total box mass was used as mass of "active" material. On the other hand, plastics was considered to be fairly "non-active" in these processes and only a small fraction of box mass was used (search for optimal fraction is discussed later with the final MLR model):

$$\text{mass of "active" material} = \begin{cases} \text{for non} - \text{plastic boxes:total box mass} \\ \text{for plastic boxes:fraction of total box mass} \end{cases} \qquad (11)$$

Note that both predictors were constructed so as to have the same unit, i.e., day⁻¹:

$$\text{AER/MSI} = \left[\frac{1}{\text{day}} \times \frac{\text{g}}{\text{g}}\right] = \left[\text{day}^{-1}\right], \qquad (12)$$

$$\text{WVTR/MSD} = \left[\frac{\text{g}}{\text{m}^2\text{day}} \times \frac{\text{m}^2}{\text{g}}\right] = \left[\text{day}^{-1}\right]. \qquad (13)$$

The rescaled parameter, Humidity Attenuation (HA) index, was calculated with min-max rescaling (with central inversion) as follows:

$$\text{HA index}^i = (1 - \frac{s^i - \ \min(s)}{\max(s) - \ \min(s)}) \times 100 \qquad (14)$$

In addition, the two predictors were standardized so that their distribution had the properties of a standard normal distribution with a mean of 0 and a standard deviation of 1, as follows:

$$\left(\text{AER/MSI}\right)_{\text{stand.}}^i = \frac{\left(\text{AER/MSI}\right)^i - \text{Mean}\left(\text{AER/MSI}\right)}{\text{Std.Dev.}\left(\text{AER/MSI}\right)}, \qquad (15)$$

$$(WVTR/MSD)^i_{stand.} = \frac{(WVTR/MSD)^i - Mean(WVTR/MSD)}{Std.Dev.(WVTR/MSD)}.$$

(16)

Results
Simple one-parameter model

In addition to the characteristics defined in section 2, an important aspect in evaluating storage performance is the microclimate inside the box and the extent to which the box can dampen the internal RH. In this context, it is desirable that the microclimate (especially RH) is as stable as possible regardless of external conditions. We are interested in the capacity of the boxes to dampen the relative humidity within the box when exposed to varying external relative humidity conditions, which we further call the RH damping capacity. A small or negligible RH damping capacity would mean that even small changes in external RH would be immediately reflected in internal RH as if the box were opened. On the other hand, changes in internal RH would be small and slow compared to externally forced changes in RH for boxes with high RH damping capacity. Models describing moisture and heat transport are of great importance for a better understanding of the materials and design of boxes that would be suitable for long-term storage of important heritage objects. There are several modelling approaches to achieve this goal. They range from detailed white box models, which provide an (almost) complete description of the physical processes under near-ideal conditions, to very simple empirical models, which disregard several details and focus on the accurate description of the available experimental data.

Our goal in the first part of the study was to analyze measurements of RH that were made for diverse set of boxes and to try to find a modelling approach that would provide a quantitative measure of the "RH damping capacity" of the boxes. We wanted our model to be generally applicable to different experimental conditions, materials and types of box constructions.

Here we present a very simple empirical model capable of adequately describing the RH fluctuations within the microenvironment of a box relative to the external RH fluctuations. The model is as simple as possible and contains only one parameter "s" to describe complex moisture and heat transport processes. This, of course, means that we are very limited in interpreting the mechanistic aspects and some of the quality of the prediction is also lost, but the model allows us to determine the parameter s of the boxes, unique for the specific box and the tested range in environmental (RH and T) conditions, which can be used to compare the RH damping capacity of the boxes.

Table 2 and Fig. 2 summarize the parameter s determined for each box group. First, it is noticeable that the parameter s is scattered by more than 3 orders of magnitude, from 5.7E-5 to 1.3E-1. The wide scatter of the s values is nicely illustrated by the box diagram inserted in Fig. 2, where the logarithmic s values are plotted. Moreover, "Kraft" group consists of only two boxes, so the maximum s-value in Table 2 thus refers to "A4 Kraft wrap" and the minimum s-value refers to "A4 Kraft wrap PE". For this reason, both boxes are also annotated in Fig. 2. In general, boxes with smaller parameter s have a better RH damping capacity and thus better moderate RH inside the box versus outside and vice versa. For example, comparing the direct RH measurements for the boxes in Fig. 3, it is obvious that the boxes "NUK lineco glue" and "A4 CLAMss JPP1 Moistop" (bottom) dampen external RH much better than the boxes "IKS_WP821" and "A4 2-P GL JPP1 sealed E" (top). This qualitative observation is quantified by the value of the parameter s. Here, the calculated s values are 2.5E-4 and 5.7E-5 versus 4.6E-3 and 2.5E-3, respectively. Note also that the model is able to distinguish between corrugated WP821 (s = 4.6E-3) and non-corrugated JPP1 box (s = 2.5E-3). The results show that corrugated WP821 board (Fig. 3, top-left) has a worse RH damping capacity than non-corrugated JPP1 board (Fig. 3, top-right), although this is not immediately visible in the graphs due to the different time scales. This is also the case when comparing the median s values between the two groups, with 6.4E-3 versus 3.1E-3 (Table 2). Microperforated plastic boxes (besides Kraft) have significantly higher s-values than boxes in other groups (median s-value = 1.1E-1), indicating that these boxes have very poor RH damping capacity. On the other hand, boxes in the "Cardboard-Coated/ > 1 mm" group have significantly lower

Table 2 | Summary of parameter *s* for empty and unstacked boxes grouped by type of box

	Median	Min	Max	N
Cardboard-Coated/ > 1 mm	3.2E-4	5.7E-5	2.6E-3	9
Cardboard	3.1E-3	2.3E-3	3.6E-3	11
Cardboard-Flute	6.4E-3	4.6E-3	1.7E-2	13
Plastic	9.2E-3	5.5E-3	1.5E-2	9
Plastic-Microperforated	1.1E-1	7.8E-2	1.3E-1	4
Kraft (w/o PE)		2.0E-3	5.3E-2	2

Fig. 2 | Summary of parameter *s* for empty boxes grouped by type of box and displayed as box plots. Box plot inserted in top left corner shows the distribution of log *s* values for all the boxes.
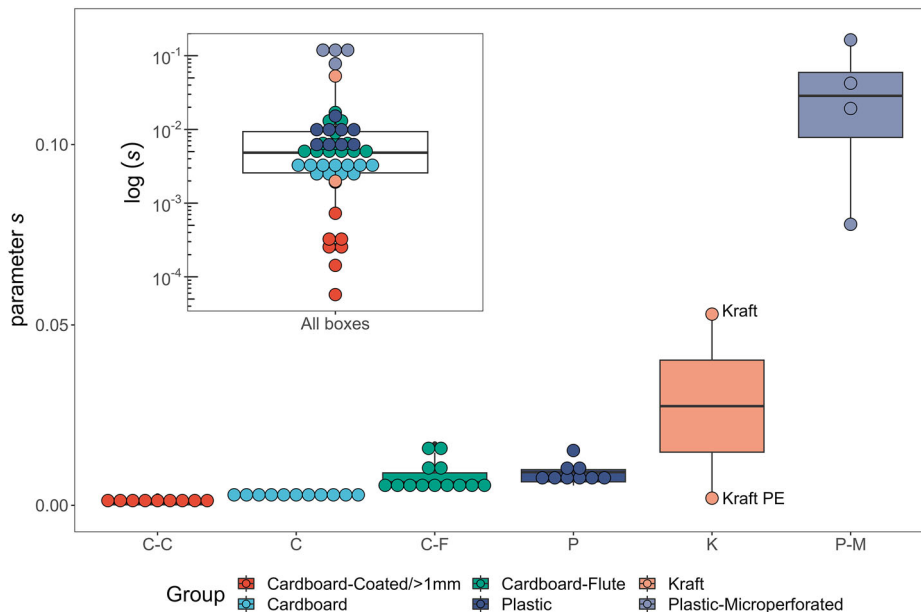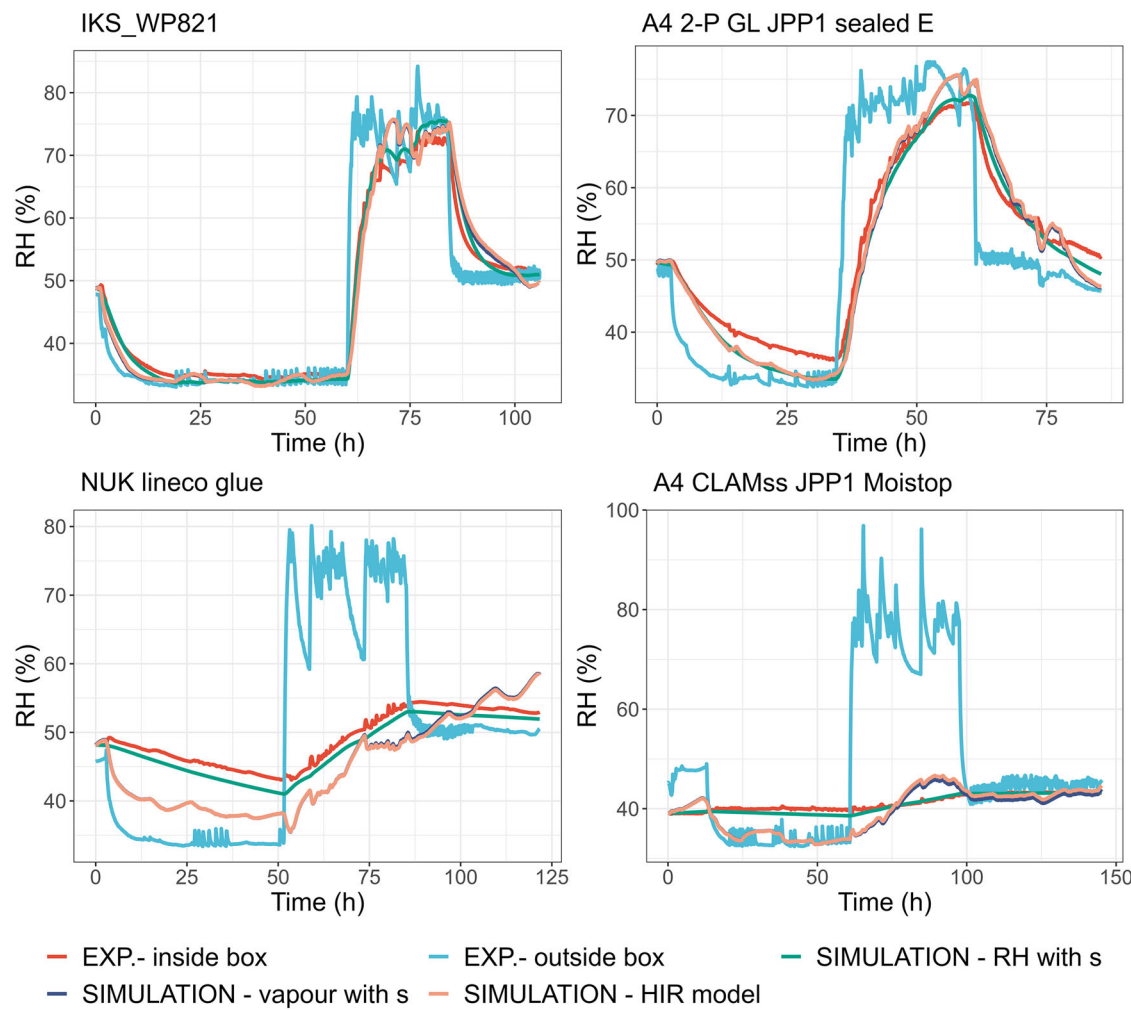
Fig. 3 | Relative humidity time series for four representative enclosures. These show the comparison between the RH predictions achieved via the one-parameter models based on RH (Eq.(1)), the one-parameter model based on vapour pressure (Eq.(6)) and the effective capacitance model including the HIR-value (Eq.(7)): top left: corrugated cardboard WP821 with CLAMls design (s = 4.6E-3); top-right: non-corrugated JPP1 cardboard with 2-P design and with sealed slits using self-adhesive tape (s = 2.5E-3); bottom-left: cardboard with textile lining (Solander box), made with LINECO glue (s = 2.5E-4); bottom-right: JPP1 cardboard coated with Moistop (s = 5.7E-5). Note that the results of the one-parameter model based on vapor pressure and the effective capacitance (HIR) model overlap significantly.

s-values compared to boxes in other groups (median s-value = 3.2E-4), indicating that these boxes have a very high RH damping capacity on average. A complete set of the calculated s-values is shown in Table SM6.

Moisture and heat transport can occur not only through the walls of the boxes, but also through holes in the walls and small slits. To determine the effect of the latter on the RH damping capacity, we tested different box designs: with and without holes, sealed and unsealed slits, use of glue, 2-part vs. CLAM. The results show that at low air velocities (0.02 m/s), no significant differences in RH damping capacity were observed for the same type of material. This suggests that the primary and by far the most important mechanism for moisture transport (at least at low air velocities) is through the walls of the boxes.

In general, a model can either be too simple, resulting in data that is underfitted leading to bias in prediction, or the model can be too complex, containing too many variables to be fit. The latter leads to overfitting of the available data and modelling also noise in the data and consequently a large variance in the prediction. Our modelling approach is very simple and includes only one parameter (s). However, the calculated RMSE for the experimental values compared to the predicted RH in a box in Fig. 4 suggest that the modelling uncertainty is in the range of the expected experimental uncertainty. The RMSE is below 3% for all boxes (red line), with the median RMSE being 1.7%, except for Kraft PE box. In other words, the model is able to predict RH within the box with less than 3% error on average. How does

this compare to experimental uncertainty? There are several sources of experimental uncertainty in the measurement of RH. The most obvious is logger accuracy, although it is not necessarily the largest contributor to the overall experimental uncertainty. If we consider only logger accuracy, which is ±2.5%, we can conclude that the one-parameter model adequately describes the changes in RH within the box. This suggests that adding additional parameters to the model would most likely result in overfitting the data, or as Occam's razor principle states, "entities should not be multiplied without necessity." Visualization of experimental and modelling uncertainty is shown on an example for corrugated cardboard in Fig. 5 with uncertainty bands of 2.5 and 3%, respectively.

The quality of the model was also assessed by statistical comparison of the calculated s values from repeated measurements for the same box (Table 3), which provided an estimate of the overall expected uncertainty. Replication analysis was performed for five different JPP1 boxes and one box from EcopHant ("A4 CLAMls GL Recy E"). These boxes have similar RH damping capacity with s values ranging from 2.3E-3 to 4.4E-3. Based on the calculated relative standard deviation (RSD) for each box, we can estimate that the overall uncertainty is less than 20%. This value includes (slight) differences in experimental (external RH) boundary conditions and is within the range of expected overall experimental uncertainty.

There are few potential problems arising from the "simple" black box modelling approach. Since temperature is not considered in the modelling,

Fig. 4 | Evaluation of modelling uncertainty using Root Mean Square Error (RMSE) by group and together. The red line is drawn at 3% RMSE.
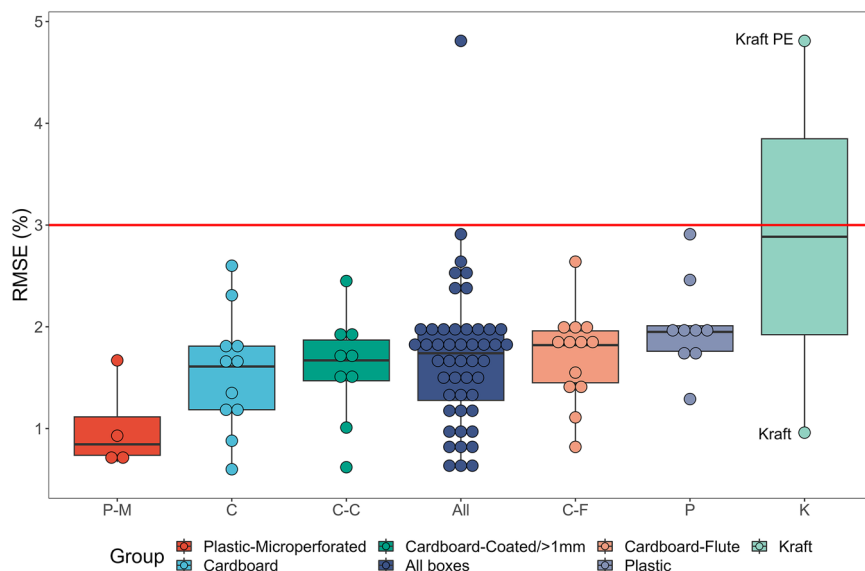

Fig. 5 | Visualization of experimental (for RH inside and outside) and modelling uncertainty (for predicted RH inside) for corrugated cardboard (box code: IKS_WP821). The uncertainty bands are ±2.5% and ±3% for experimental and modelling uncertainty, respectively.
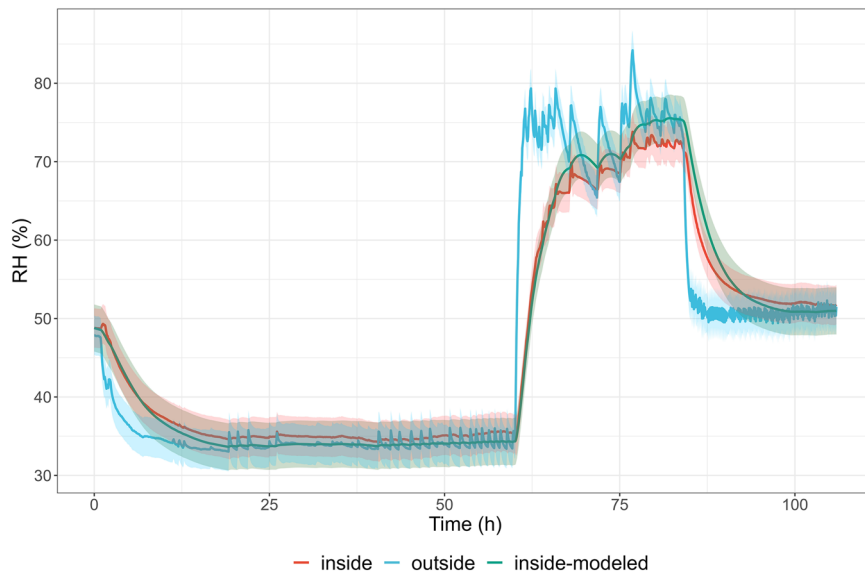
one such risk could be a sudden drop in external temperature which in reality could lead to condensation inside a box if the box is sealed and moisture transport is limited (e.g., fully sealed plastic boxes)[25]. This type of box could theoretically have a good RH damping capacity with a small s-value, however, would obviously not be suited as a storage enclosure in a museum. Also, the RH damping capacity is expected to be influenced by the range in environmental relative humidity, as the hygric properties (MSI, WVRT) are a function of relative humidity. However, within the interested range in RH, we expect this impact is limited.

Predicting the RH damping capacity using material/box properties

The parameter s, resulting from an empirical one-parameter model and direct RH measurements, can be considered a unique indicator of the RH damping capacity of the boxes. To better understand this complex parameter, various material and box properties were measured. As can be seen in the scatter plots of each pair of material/box properties with the parameter s in Fig. SM9, no single property is a good predictor of the parameter s. Interestingly, AER and WVTR are highly correlated properties with a Pearson correlation of 0.842 (as seen in Fig. SM9). However, both properties

are good predictors of the parameter s when only non-plastic or plastic boxes are included - we see two separate linear trends with smaller slope for plastic boxes and larger slope for non-plastic boxes. To bring these two separate trends together two new predictors were constructed and combined to form a multiple linear regression (MLR) model to predict the parameter s, see Eq. (9).

Both predictors in the MLR model are constructed by the quotient of two properties. First, AER is divided by the moisture sorption isotherm - MSI (AER /MSI), which means that AER is directly proportional to its MSI. AER represents dry diffusion of CO_2 through the porous material with limited interaction of CO_2 in box walls. AER is highest for corrugated cardboard boxes. In addition, microperforated plastic allows much faster diffusion compared to non-microperforated plastic, which also results in higher AER. This is an important property of plastic material for the RH damping capacity, as we will see in the Discussion section. However, for some boxes, not only the type of material but also the design is an important factor for AER. For example, if a box cannot be sealed tightly, AER will tend to be higher, as in the case of "A4 CLAMls GL Recy E" and "A4 CLAMls CL JPP1.3 E". MSI, on the other hand, depends on equilibrium due to hydrogen bonding and provides information about the material's ability for absorbing

Table 3 | Results of replicate measurements for selected boxes

Box code:	A4 CLAMss CL JPP1 H E	A4 CLAMss CL JPP1 E	A4 2-P GL JPP1 H E	A4 2-P GL JPP1 E	A4 CLAMls GL Recy E	A4 2-P GL JPP1 sealed E
N	2	10	4	4	2	2
mean 's'	3.57E-03	3.40E-03	3.30E-03	2.77E-03	2.59E-03	2.52E-03
max 's'	3.94E-03	4.39E-03	3.96E-03	3.15E-03	2.77E-03	2.70E-03
min 's'	3.19E-03	2.43E-03	2.65E-03	2.50E-03	2.41E-03	2.34E-03
RSD [%]	14.8	18.5	18.1	11.8	9.9	10.2

water with each unit increase of RH. MSI is not dependent on the design of the box, so all plastic boxes (regardless of microperforation) have a very small MSI. This means that plastic boxes have the largest AER /MSI values compared to other boxes, although microperforated boxes have significantly larger AER /MSI values than non-microperforated boxes due to the larger AER.

The second predictor was formed from the WVTR, the mass of the box, and the outer surface area of the box. WVTR represents water vapour transport through a material in a unit of surface area and time at fixed temperature and RH[26]. WVTR and MSI are not correlated properties with Pearson correlation coefficient equal to 0.375, Figure SM9. For example, both boxes made from Kraft paper ("A4 Kraft wrap PE" and "A4 Kraft wrap") have a large and similar MSI (0.1050 and 0.1070, respectively), but completely different WVTR values (13.5 g/m²/day and 1892 g/m²/day, respectively). The reason for the observed differences is that WVTR is a measure of the kinetics of water transport through box walls, while MSI (slope) is a measure of change of moisture content of box walls in a specified RH interval. For this reason, coated boxes have a much lower WVTR as in the above example of boxes made from Kraft paper[27–29]. Similarly, non-microperforated plastic boxes will also have a negligible WVTR. This is also why WVTR and AER are highly correlated properties (Pearson correlation coefficient is 0.842). To create a predictor similar to the first (AER /MSI), WVTR was divided with the "Material Surface Density" (MSD), which is actively involved in the interactions with water molecules in the gas phase. Here, a simple mono-layer wall is assumed which uniformly stores water and heat. The MSD was calculated by dividing the mass of the "active material" by the outer surface area of the boxes, see Eqs. (10–13).

Discussion

The ideal parameter to characterise buffering in a preventive conservation context needs to fulfil two conditions: firstly, it should refer to RH (rather than absolute humidity or temperature), because it is the most interesting quantity for conservation outcomes. Secondly, the ideal buffering parameter should be obtainable from real-world time-series of T and RH, ideally measured hourly. This is because this is the data type most widely available from museums. Any museum who owns two humidity loggers can use them to conduct buffering experiments by placing one inside and one outside an enclosure, without the need of acquiring more sophisticated equipment[19]. In section 3.1 a simple one-parameter model based on RH was applied. Other models could however be chosen. The one-parameter RH-model expressed in Eq.(1) is compared with (a) a one-parameter model based on the vapour pressure difference and (b) the effective capacitance model[21], see respectively Eqs.(6–8).

Several standardized methods are used to measure the MBV, including the Nordtest Protocol[30], ISO 24353[31], and JIS A 1470[32]. The Nordtest Protocol is one of the most widely adopted methods, involving cyclic exposure of a material sample to alternating high and low RH levels (e.g., 75 and 33% RH) under controlled conditions, with each cycle typically lasting 8 h. The MBV is calculated from the measured mass change of the sample during these cycles. In addition to these standardized approaches, field methods can estimate HIR by analyzing T and RH time series from real-life environments, correlating observed RH fluctuations with the material's moisture exchange[33]. Further research to apply these methods in the museal or collection context is however needed. HAM (Heat, Air and Moisture) models,

on the other hand, provide a more comprehensive approach[34]. These models couple heat and moisture transfer processes in porous materials by solving partial differential equations for energy and mass conservation. While theoretically all these options can extract useful information from T and RH data of real-world enclosures, the more complex the model, the more input parameters it needs to run. Figure 3 shows a comparison of the relative humidity predictions achieved based on the simple relative humidity model (Eq.(1)), vapour pressure model (Eq.(6)) and effective capacitance model (Eq.(7)). Consistently, the simple one-parameter model based on RH offers a better prediction of the internal RH than the effective capacitance model, or the one-parameter model using the vapor pressure. This better performance is especially true for the box made out cardboard with textile lining (Solander box) made with LINECO glue and the box made out JPP1cardboard coated with Moistop, which both have a higher RH damping capacity. For the purposes of this paper it is clear that the simple one-parameter RH model provides sufficiently good predictions to obtain fitting parameters for each enclosure, that can be used for further analysis of their buffering properties.

The parameter s can be used as an indicator of the RH damping capacity of the boxes, and although the experiments were performed under different relative humidity conditions, the calculated s-value is, within the RH range of interest, unique to the specific box. A relative error below 20% is found for this s-value, taking into account limited external RH variations (Table 3). However, all comparisons between the s-values of the boxes are relative in the sense that we have no reference box with which to compare the results. That is, we do not know at what RH damping capacity (i.e., what parameter s) we might consider a box to be a "suitable box". It is clear that the box "A4 CLAMss JPP1 Moistop" (Fig. 3, bottom right) has sufficient RH damping capacity, but this is not the case for the boxes "IKS_WP821" and "A4 2-P GL JPP1 sealed E" (Fig. 3, top). It is therefore necessary to imagine a test environment for which the internal RH can be calculated for each box based on its given parameter s. We have constructed a hypothetical Low-Quality Environment (LQE, Fig. 6, red line) in which the daily RH fluctuations are between 30 and 80%. This simulates very poor storage conditions, such as we would find in old churches, castles, or similar poorly insulated buildings[34–37]. Once we had calculated the internal RH for each box exposed to LQE, we still needed a second hypothetical environment to which we could compare the performance of the boxes. This second environment represents what we call a Medium Quality Environment (MQE, Fig. 6, green line), a minimum storage requirement that we would consider appropriate in terms of preservation. We assumed that acceptable daily RH variations (MQE) ranged from 45 to 65%. Thus, the criteria for evaluating the suitability of a box are simple: if the fluctuations in predicted RH in a box (at LQE) are equal to or less than the fluctuations of RH in a MQE, the box is considered to have sufficient RH damping capacity. The decision criteria can be quantified by the difference (Diff) between the simulated maximum RH within a box (Fig. 6, blue line) and the maximum RH in the MQE. The Diff parameter is calculated after 72 h, when the equilibrium of RH within a box is reached, and by definition ranges from −10% for boxes with an ideal RH damping capacity to +15% for boxes with very poor RH damping capacity ("open" boxes). Boxes for which the Diff parameter is less than or equal to 0% are considered "suitable boxes" in terms of their RH damping capacity. An example of the calculation of the Diff parameter for a hypothetical box with an s-value of 0.005 is shown in

Fig. 6 | Assessing the RH damping capacity. An example of assessing the RH damping capacity for a hypothetical box with parameter $s = 0.005$ when exposed to hypothetical Low-Quality Environment (LQE) and compared to Medium-Quality Environment (MQE).
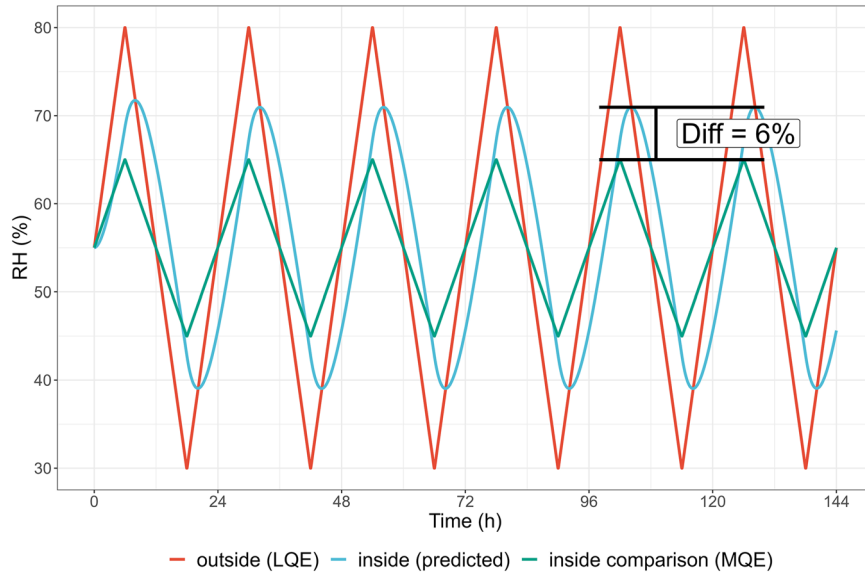

Fig. 6. Based on the criteria established, this box with a Diff value of 6% does not have sufficient RH damping capacity.

The suitability of the RH damping capacity of the boxes can be shown in a simple 2D plot with the parameter Diff versus the logarithmic value of s for each box (Fig. 7). The relationship is sigmoidal and gives a clear representation of the grouping of boxes by RH damping capacity. "Suitable boxes" have Diff less than or equal to 0% (i.e., s values $\leq 2.5E\text{-}3$), which is shown with green shading in Fig. 7. In addition, based on the uncertainty analysis of the final MLR Model 6 (discussed in the preceding section), boxes with Diff between 0% and 3.4% ($2.5E\text{-}3 < s < 3.70E\text{-}3$) can be classified as "Likely suitable boxes" (shaded grey). These two categories include all boxes in the following two groups: "Cardboard-Coated/ >1 mm" and "Cardboard", with the addition of "A4 Kraft wrap PE". Boxes with a Diff value greater than 3.4% ($s > 3.70E\text{-}3$) can be considered as boxes with poorer RH damping capacity, although there is a clear distinction between them. Corrugated cardboard boxes ("Cardboard-Flute") and non-microperforated plastic boxes ("Plastic") have a significantly better RH damping capacity than "A4 Kraft wrap" and microperforated plastic boxes ("Plastic-Microperforated").

Using Eq. 9 and Eq. 10, we calculated the regression parameters for 48 empty and unstacked boxes (also used in the previous section). The results shown in Figure SM10 confirm that the MLR with constructed predictors is suitable for describing parameter s. Most of the boxes have s values lower than 0.02, except for the microperforated plastic boxes ($0.13 > s > 0.08$) and the "A4 Kraft wrap" box ($s = 0.053$). To get a better understanding into the RH damping capacity of these boxes, we can calculate the internal RH when exposed to LQE, and further calculate the Diff parameter when compared to MQE. This is shown in Figure SM11 for the "A4 Kraft wrap" box. Since microperforated plastic boxes have an even larger s-value, we can conclude that boxes with an s-value greater than 0.05 can be treated as "open" boxes with little to no damping capacity. These boxes were therefore removed from further modelling attempts.

Notwithstanding the fact that we focus only on the relevant range of the parameter s, we are still dealing with a very large range from $5.7E\text{-}5$ to $2.0E\text{-}2$, i.e., almost 3 orders of magnitude. This makes an intuitive comparison of the RH damping capacity between boxes difficult. To improve this, a normalization or min-max scaling (with central inversion) of the parameter s to a fixed range between 0 and 100 was performed, see Eq. (14). The rescaled parameter was renamed to a Humidity Attenuation (HA) index. Table 4 lists statistical parameters of six MLR models with HA index as an outcome and standardized predictors with different boxes and variables included. Note, however, that these transformations do not change the data distribution or

the statistical parameters of the MLR models. This can be seen by comparing Fig. SM12, where the parameter s was used as the outcome, with Fig. SM13, where the HA index was used instead and predictors were standardized (Table 4, Model 1). Because of the central inversion, the data points are now reflected so that, for example, data points that were previously in the lower bottom corner now appear in the upper right corner and are also on the opposite side of the $y = x$ line.

In general, the HA index (parameter s) is a convenient tool for summarising complex information in a single number. It provides a simple way to compare the buffer capacity of two boxes. The HA index measures how well the box dampen RH inside the box relative to the fluctuations outside, on a scale of 0 to 100. However, the HA index has no intrinsic meaning; it is a comparison tool. A box with a very good RH damping capacity - outside fluctuations have little effect on RH inside the box - would have a HA index of 100 or close to it. In contrast, a box in which changes in RH inside the box are instant relative to external RH would have a HA index equal to or close to 0. Based on the RH damping capacity assessment of the boxes (simulation when exposed to LQE and compared to MQE), the range between 0 and 100 can be divided into three categories (as before), which are also shown in Fig. SM13 as three shaded areas, similar to Fig. 7. "Suitable boxes" have a HA index greater than or equal to 85.8 (Fig. SM13, shaded green), and based on the uncertainty in the MLR model (discussed later), boxes can be classified as "Likely suitable" if the HA index is between 78.5 and 85.8 (Fig. SM13, shaded grey). Boxes with an HA index less than 78.5 have poorer buffer capacity (Fig. SM13, shaded red). Additionally, horizontal and vertical dashed red lines are inserted at the decision point with HA index equal to 85.8.

The purpose of archival boxes is, of course, preservation of objects such as a range of documents, photographs, textiles, art and more. These objects can indeed affect the RH damping capacity. In our case study, we filled four boxes of non-corrugated cardboard and one box of corrugated cardboard with standard printing paper and examined the impact on the RH damping capacity. We would expect the RH damping capacity to increase for such boxes because the added paper can buffer (adsorb/desorb) moisture. The MLR model described above can be extended to include this type of scenario by simply adding the mass of paper to the mass of "active" material. This leads to an increase in MSD and a decrease in the second predictor "WVTR/MSD", which in turn increases the HA index. The results of predicting the HA index for "filled" boxes are shown in Fig. 8A (also Table 4, Model 2). Considering the simplicity of the model, the predictions for filled boxes have relatively good accuracy, although the absolute error for "A4 CLAMls CL JJPflut" is nevertheless large (the residual is 14). As expected, boxes filled

Fig. 7 | Evaluation of boxes' RH damping capacity.
Boxes with *Diff* < 0% and 0 < *Diff* < 3.4% can be considered "suitable boxes" and "likely suitable boxes", respectively. Boxes with poorer RH damping capacity have *Diff* > 3.4%.
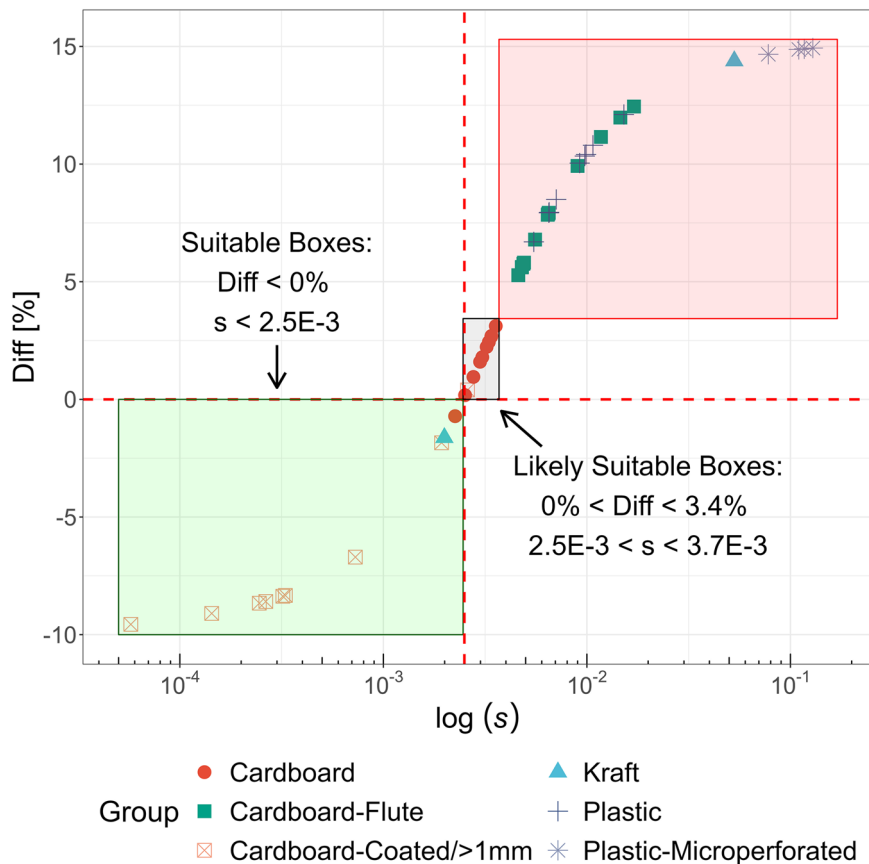
with paper have better RH damping capacity, as the HA index increases by 17% on average compared to empty boxes (the average increase when calculated from MLR model is 13%, Table 5). The increase in RH damping capacity means that cardboard boxes which were previously categorized as "likely suitable" are now "suitable". The most profound effect is seen for corrugated box "A4 CLAMls CL JJPflut" with 57% increase in HA index (37% when predicted by MLR model) and the RH damping capacity changes from "poor" to "suitable" as a result of adding paper.

In our second case study, we stacked empty boxes on top of each other to simulate a more realistic scenario in storage areas. This meant that the external surface area directly exposed to external conditions decreased, as only the side surfaces were exposed. The MLR model also accounts for this scenario by simply correcting the external surface area of the box to account for the actual area directly exposed. The consequences are similar to filled boxes, the MSD increases, the second predictor "WVTR/MSD" decreases, and a larger HA index is calculated (Fig. 8B). The model adequately accounts for stacking with no obvious outliers (Table 4, Model 3). Stacking boxes increases HA index by 17% on average and by 9% when predicted by the MLR model (Table 5). A special case here is the coated cardboard box "A4 2-P GL JPP1 coated", which has a very good buffering capacity (HA index is 99.5) and stacking has limited effect. The results suggest that filling boxes with paper or stacking boxes on top of each other significantly improves the RH damping capacity, but for different reasons. Added paper increases the potential to buffer moisture, while reducing the available surface area limits water permeability through the walls. Interestingly, the effects of these two processes (buffering versus permeability) are similar but opposite.

In the last step of model development, we used all available data. This includes empty (43), filled (5), and stacked (5) boxes, for a total of 53 boxes. To test the significance of the two predictors, we created two simple linear regressions with one parameter. The first regression (Table 4, Model 4) included only $(AER/MSI)_{stand.}$ while for the second regression we included

$(WVTR/MSD)_{stand.}$ (Table 4, Model 5). Indeed, both predictors show a significant correlation with the HA index when used separately, with an R-squared of 0.4868 and 0.5946 for Model 4 and Model 5, respectively. Model 4 with $(AER/MSI)_{stand.}$ is particularly good at predicting the HA index for non-microperforated plastic boxes ("Plastic" group), while a better correlation for corrugated and noncorrugated cardboard boxes ("Cardboard" and "Cardboard-Flute" groups) was obtained in model 5 with $(WVTR/MSD)_{stand.}$ (cf. Figures SM14, SM15). When both predictors are included in a regression, the correlation is much better with both regression coefficients significantly different from zero ($p < 2E-16$), and multiple R-squared and standard error of the residuals of 0.9392 and 6.256, respectively (Table 4, Model 6). In addition, we can test whether the relationship between one predictor and the HA index depends on the level of the other predictor, that is, whether the relationship between one predictor and the HA index is independent of the other predictor variable. The results of an MLR model with interactions suggest that the interaction parameter between $(AER/MSI)_{stand.}$ and $(WVTR/MSD)_{stand.}$ is not significant ($p = 0.435$). This means that we can use MLR model 6 (without interactions) and interpret the effects of each predictor on the outcome independently. For example, an increase of 1 (equal to one standard deviation in the predictor distribution) in $(AER/MSI)_{stand.}$ is associated with a decrease of 14.77 in the HA index when controlling for $(WVTR/MSD)_{stand.}$. However, both predictors have a similar effect on the HA index, as the regression coefficient for $(WVTR/MSD)_{stand.}$ is -16.92 – a difference in increase of only 2.15.

An important parameter in the MLR model is the MSD and the mass of the material actively involved in the thermohygrometric processes. As mentioned earlier, the mass of "active" material for non-plastic material was estimated as the total mass of the box, while for plastic boxes only a small fraction of the total mass of the box is actively involved in these processes. The mass of "active" material for non-microperforated plastic boxes was determined by calculating a multiple regression (Model 6) with the highest R-squared value at different fractions of the total box mass. The optimal

Table 4 | Comparison of statistical parameters of MLR models with HA index as an outcome and standardized predictors

	Model 1	Model 2	Model 3	Model 4	Model 5	Model 6
Boxes included in the model	Empty (unstacked) Boxes	Empty&Filled (unstacked) Boxes	Empty&Stacked Boxes	Empty&Filled& Stacked Boxes	Empty&Filled& Stacked Boxes	Empty&Filled& Stacked Boxes
Number of boxes	43	48	48	53	53	53
(Intercept)	69.7963	72.7933	72.6777	75.1200	75.1200	75.1202
Std. Error	0.9565	0.9387	0.8781	2.471	2.196	0.8593
$Pr(>|t|)$	<2E-16	<2E-16	<2E-16	<2E-16	<2E-16	<2E-16
$(AER/MSI)_{stand.}$	−15.6872	−15.1213	−15.3642	−17.3520		−14.7719
Std. Error	0.9713	0.9551	0.8950	2.495		0.8778
$Pr(>|t|)$	<2E-16	<2E-16	<2E-16	6.41E-9		<2E-16
$(WVTR/MSD)_{stand.}$	−16.8443	−17.1988	−16.7644		−19.177	−16.9257
Std. Error	0.9713	0.9551	0.8950		2.217	0.8778
$Pr(>|t|)$	<2E-16	<2E-16	<2E-16		1.43E-11	<2E-16
Residual Std. Error	6.272	6.503	6.083	17.99	15.99	6.256
Multiple R-squared	0.9387	0.9353	0.9428	0.4868	0.5946	0.9392
p-value	<2E-16	<2E-16	<2E-16	6.415E-9	1.429E-11	<2E-16
RMSE	6.0496	6.2969	5.8902	17.6483	15.6855	6.0760
$RMSE_{LOOCV}$[a]	7.4606	7.5156	7.1708	18.2351	16.2365	7.2047
$RMSE_{repeated\ k-fold\ CV}$[b]	7.6143	7.6142	7.3146	18.2972	16.3497	7.2912

[a]RMSE – Leave-One-Out Cross-Validation.
[b]RMSE – 500 repetitions, data split into 5 groups (folds).

Fig. 8 | Comparison of affect of filling or stacking boxes on RH damping capacity. Analysis of (**A**) boxes filled with paper (MLR Model 2, Table 4) and (**B**) boxes stacked with paper (MLR Model 3, Table 4) on RH damping capacity.
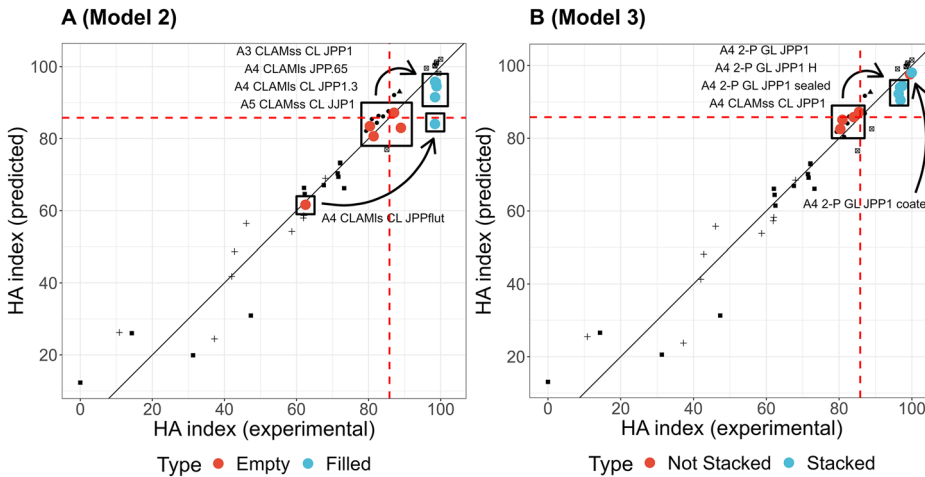
fraction was found to be 0.814% (Fig. SM16). This fraction was used in all calculations.

The final MLR model 6 was validated with Leave-One-Out Cross-Validation (LOOCV) and repeated k-fold cross-validation (k-fold CV). The RMSE for repeated k-fold CV was calculated by randomly splitting data into five equal-sized groups (folds) and repeating the procedure 500 times. LOOCV and the repeated k-fold CV yield similar results, with an RMSE of 7.205 and 7.291, respectively (Table 4, Model 6). The results show that the prediction of the HA index differs on average by 7.3 from the actual HA index. Thus, the uncertainty of boxes at Diff = 0% will be HA index = 85.8 ± 7.3. It follows that a box with HA index between 78.5 and 85.8 can be considered a "likely suitable" box, considering the uncertainty (Fig. 9, shaded grey). The result of the final MLR model 6 is shown in Fig. 9.

For some coated cardboard boxes model predicts HA indices above 100, which is above the defined range of the HA index. These boxes include:

NUK boxes (from 100.7 to 101.8) and cardboard boxes coated with Moistop (102.6) and EVA (100.1). However, these predictions are not surprising considering the large "experimental" HA indices (NUK - from 98.4 to 98.9; Moistop - 100; EVA - 96.0) and model uncertainty. It is also important to remember that the range of the HA index is defined based on the data set used. Here, the upper limit is defined as the RH damping capacity measured for the box "A4 CLAMss JPP1 Moistop". In general, a prediction of the HA index close to or just above 100 (± 7.3) indicates a very good RH damping capacity. Such boxes can be considered as almost completely sealed boxes with an internal microenvironment that is well isolated from the fluctuations of the external environment RH.

Regression diagnostics was also performed to assess outliers, influential data points, and heteroscedasticity. Outliers, i.e., extreme values whose experimental HA indices were far from most of the other predicted HA indices, were examined using the standardised residuals (residual divided by

Table 5 | Comparison of increase of HA index for boxes filled with paper or stacked boxes (in %)

Box code	Comparison	From experimental data	Predicted by MLR model
A3 CLAMss CL JPP1	Empty vs. Filled	23	13
A5 CLAMss CL JPP1	Empty vs. Filled	13	10
A4 CLAMls CL JPP.65	Empty vs. Filled	21	19
A4 CLAMls CL JPP1.3	Empty vs. Filled	11	10
	Average =	**17**	**13**
A4 2-P GL JPP1	Empty vs. Stacked	15	10
A4 2-P GL JPP1 H	Empty vs. Stacked	19	9
A4 2-P GL JPP1 sealed	Empty vs. Stacked	14	8
A4 CLAMss CL JPP1	Empty vs. Stacked	21	10
	Average =	**17**	**9**
Special cases:			
A4 CLAMls CL JPPflut	Empty vs. Filled	57	37
A4 2-P GL JPP1 coated	Empty vs. Stacked	0.5	0.5

Separate averages are calculated from experimental data and data predicted by the MLR model for comparison between empty vs. filled and empty vs. stacked, respectively. Two special cases were not included in the calculation of averages.

the standard error of the residuals). Although a value may not be an outlier, it may still be an influential value with high leverage, the absence of which would significantly alter the regression equation. High leverage values were determined by evaluating hat values and Cook's distances. Both outliers and high influential values were analysed using the influence diagram shown in Fig. SM17. For standardised residuals, two vertical dashed lines are drawn at ±2, indicating outliers that are two or more standard errors away from the regression line. Data points are potentially influential if their leverage values are more than (2 or) 3 times greater than the mean leverage value (0.113 and 0.170) or if Cook's distance exceeds 0.082. The circle size of the data points in the graph is proportional to the Cook distance. Data points with a Cook distance greater than 0.082 are highlighted in grey. There are only a few data points that could be considered outliers and have a large impact on the regression: four corrugated cardboard boxes WP851 and plastic boxes "ISS8DW_PP105" and "IKSDW_PP105". These boxes all have small HA indices (the predicted HA index is below 31), as shown in Fig. SM18. In addition, the plastic box "A4 2-part Prague1b" could be an influential point (based on Cook's distance) and the filled corrugated cardboard box "A4 CLAMls CL JPPflut F" has a standard residual greater than 2, suggesting an outlier. In addition, a plot in Fig. SM18 of the absolute value of the residuals versus the predicted HA indices with smoothed estimation of the relationship between the two variables ("loess" method) indicates heteroscedastic error - the variance of the residuals increases for larger HA indices. The observed heteroscedasticity suggests that the variance is not constant and the prediction error is larger for boxes with a HA index below 50. Due to the limited data set, the aforementioned data points were not removed, but caution should be taken when using and interpreting the model. The partial residual plots for the first $((AER/MSI)_{stand})$ and second $((WVTR/MSD)_{stand})$ predictor however in general confirm linear relationship between individual predictor and the HA index (Fig. SM19 and SM20), which validates linearity assumption in the MLR model.

Finally, we can use our final MLR model 6 to predict the HA index for non-microperforated plastic boxes ("Plastic") and corrugated cardboard boxes ("Cardboard-Flute") when filled with paper or stacked. The results of the predictions are shown in Fig. 10. As we have already seen, the design of cardboard boxes has no significant effect on the RH damping capacity, since the primary process by which water vapor enters and exits the box is through the walls. For double flute corrugated boxes (WP821 - EB and WP811 - FE) fluctuations reduce to the point where the predicted HA indices are above 78.5 for filled and stacked boxes. For single flute corrugated boxes (WP851 - E), we see an even more dramatic increase in predicted HA indices as the boxes are filled or stacked. Filling these boxes with paper reduces fluctuations to the point where they can be classified as "likely suitable" boxes.

Interestingly, the effect of added paper and stacking is much smaller for plastic boxes than for cardboard corrugated boxes, i.e., the absolute increase in HA index is on average 13 and 14 for plastic boxes when filled and stacked, respectively, compared to 33 and 25 for corrugated boxes. The first part of the explanation lies in the WVTR, which is very low (at the limit of determination) for plastic boxes. This means that the water vapor moves very slowly through the walls and the absorption capacity inside the box is available only up to a certain point. For example, the calculated HA index for the "A4 CLAMls Prague1a" box will only increase until about 50 g of paper is added and adding more paper will not increase the HA index any further. Note, however, that some coated cardboard boxes, e.g. "A4 CLAMss JPP1 Moistop" and "A4 2-P GL JPP1 coated E", also have a very low WVTR, but unlike plastic boxes these boxes have large HA indices (large RH damping capacity). To understand this, we need to look at the second part of the MLR equation, which is the quotient of AER and MSI (AER /MSI). For plastic boxes, MSI is again very small (at/below the limit of determination), which means that almost no water is absorbed by the walls. On the other hand, some air nevertheless penetrates through the slits and holes in the walls of the plastic boxes studied, and a relatively small AER is sufficient for the plastic boxes to have almost no RH damping capacity. The previously mentioned coated cardboard boxes "A4 CLAMss JPP1 Moistop" and "A4 2-P GL JPP1 coated E" also have relatively small AER, but in contrast to the plastic boxes have a much higher MSI. Note, however, that the HA index predicted for plastic boxes is associated with a high degree of uncertainty due to the uncertainties in WVTR and MSI determination.

In general, the models developed are as good as the data used. The MLR model presented is based on a diverse data set with various materials and box designs tested. This validates to some extent the correlations in the model. However, additional data (boxes) are needed to fully validate the model. The presented model provides a good starting point for further research, although the range of applicability needs to be better defined.

Both models presented here (i.e., the empirical one-parameter model and the MLR model) are also available as a freely available online tool, at hsll.shinyapps.io/ha_index_pub/. Currently, the app is still in the development phase (alpha version), although all calculations presented in the paper can already be performed with the app. We intend to further develop the app to support decision-making processes to engineer better enclosures.

The app can be used for two types of calculations to evaluate enclosures: first, based on direct measurements of RH fluctuations outside vs inside of an enclosure (using a one-parameter model), or second, based on experimental properties of an enclosure, i.e., enclosure size, enclosure mass, moisture sorption isotherm, water vapor transmission rate, and air exchange rate (using the MLR model).
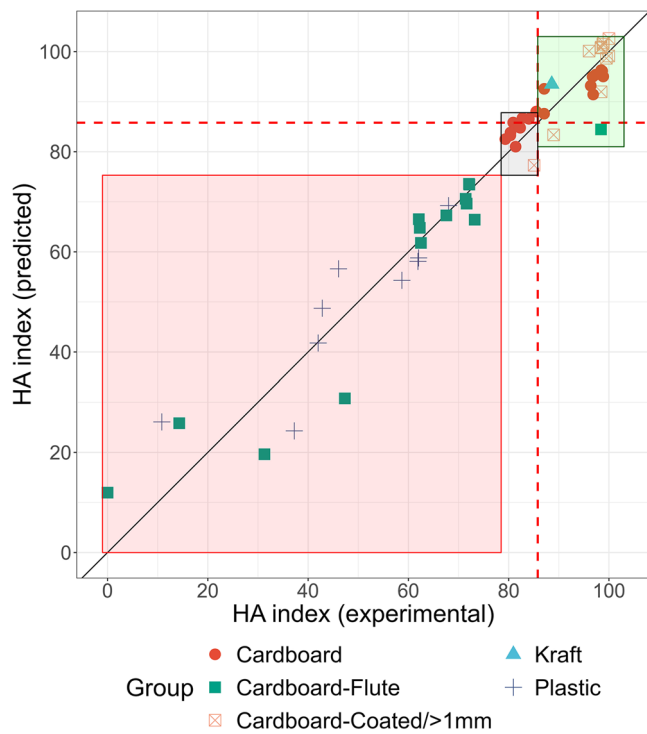
Fig. 9 | The result of the final MLR model 6. MLR model 6 (Table 4) is based on 43 empty, 5 filled boxes and 5 stacked boxes (boxes with parameter s > 0.05 removed: A4 Kraft wrap and microperforated plastic boxes (IKS_PP104, IKS6DW_PP104, ISS_PP104, ISS8DW_PP104)). Boxes can be classified into three groups according to their RH damping capacity: suitable boxes with HA index > 85.8 (green shade), likely suitable boxes with HA index between 78.5 and 85.8 (grey shade), and boxes with poorer RH damping capacity, HA < 78.5 (red shade).
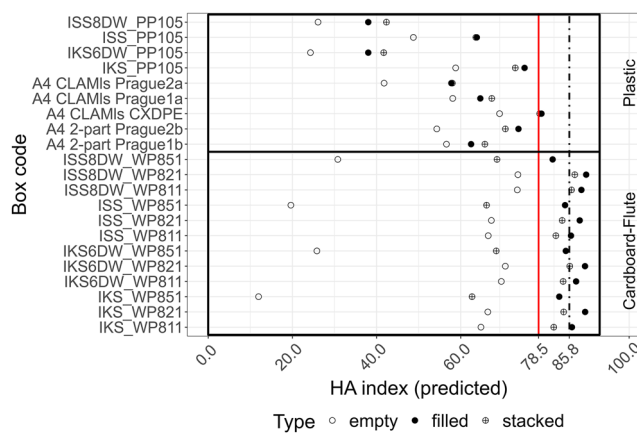
Fig. 10 | Affect of filling and stacking non-microperforated plastic and corrugated cardboard boxes on damping capacity. Prediction of HA indices using MLR model 6 for non-microperforated plastic boxes ("Plastic") and corrugated cardboard boxes ("Cardboard-Flute") if empty (empty circle), filled with paper (filled circle) or stacked on top of each other (circle cross).

This article presents a novel approach to describing microenvironments in enclosures. Complex thermohygrometric processes have been distilled into a single value, namely the HA index. The HA index is a single descriptive statistic for quantitatively describing the RH damping capacity of enclosures to moderate external RH. This statistic allows comparisons between heterogeneous groups of boxes, such as ranking storage suitability of boxes made of cellulosic fibres (paper, corrugated and non-corrugated board, and textile), plastic boards, or coated with synthetic coatings. In

addition to direct measurements from RH, the HA index can also be calculated using a MLR model based on measurable physical material-box properties. Carefully constructed regression predictors show that at low ventilation rates, the primary moisture transport processes occur through the wall (diffusive fluxes), although fluxes through holes and slits (infiltration fluxes) become important for plastic boxes. For example, poorer RH damping capacity, i.e., lower HA index, was observed for corrugated cardboard boxes (except for "A4 CLAMls CL JPPflut F"), primarily due to high WVTR values. In contrast, the low HA index for plastic boxes (especially microperforated ones) is almost exclusively due to AER. By comparing the damping capacities of boxes filled with paper and stacked boxes, we were also able to semi-quantitatively determine the absorption and permeability part of the diffusive flux. The results suggest that these two processes are important for boxes made from cellulosic fibres and appear to have a quantitatively similar but opposite effect in increasing the RH damping capacity, i.e., more available material that can buffer moisture or a smaller outer surface area of the box both lead to a higher HA index. An online app has been developed for researchers and others to evaluate the RH damping capacity of boxes in a simple and user-friendly way. In the future, we hope it can also help curators and conservators make decisions about preventive conservation measures. However, to improve the accuracy and validation of the model, the current dataset needs to be extended to other types of storage boxes and temperature measurements need to be included in the modelling approach.

Data availability

Data is provided within the manuscript or supplementary information files. Additionally, measurements of relative humidity and temperature used during the current study are available from the corresponding author on reasonable request.

Code availability

Codes generated during the current study are available from the corresponding author on reasonable request.

References

1. Duran-Casablancas, C. et al. A Comparison of Preservation Management Strategies for Paper Collections. *Stud. Conserv.* **66**, 23–31 (2021).
2. Caldararo, N. The Solander Box: Its varieties and its role as an archival unit of storage for prints and drawings in a museum, archive or gallery. *Mus. Manag. Curatorship* **12**, 387–400 (1993).
3. Smedemark, S. H., Ryhl-Svendsen, M. & Toftum, J. Distribution of temperature, moisture and organic acids in storage facilities with heritage collections. *Build. Environ.* **175**, 106782 (2020).
4. Han, B., Li, X., Wang, F., Bon, J. & Symonds, I. The buffering effect of a paper-based storage enclosure made from functional materials for preventive conservation. *Indoor Built Environ.* **33**, 167–182 (2024).
5. Rojas, A., Cabrera, F. & Corona, A. Temperature and relative humidity in a palaeontological collection: the buffering effect of microenvironments. *Ann. Paléontol.* **106**, 102446 (2020).
6. Popescu, C.-M., Hill, C. A. S. & Kennedy, C. Variation in the sorption properties of historic parchment evaluated by dynamic water vapour sorption. *J. Cult. Herit.* **17**, 87–94 (2016).
7. Kupczak, A., Bratasz, Ł., Kryściak-Czerwenka, J. & Kozłowski, R. Moisture sorption and diffusion in historical cellulose-based materials. *Cellulose* **25**, 2873–2884 (2018).
8. Brimblecombe, P. Temporal humidity variations in the heritage climate of South East England. *Herit. Sci* **1**, 3 (2013).
9. Huerto-Cardenas, H. E., Aste, N., Del Pero, C., Della Torre, S. & Leonforte, F. Effects of Climate Change on the Future of Heritage Buildings: Case Study and Applied Methodology. *Climate* **9**, 132 (2021).

10. Derluyn, H., Janssen, H., Diepens, J., Derome, D. & Carmeliet, J. Hygroscopic Behavior of Paper and Books. *J. Build. Phys.* **31**, 9–34 (2007).

11. Kupczak, A. et al. Impact of paper and wooden collections on humidity stability and energy consumption in museums and libraries. *Energy Build.* **158**, 77–85 (2018).

12. Novak, M. et al. Evaluation and modelling of the environmental performance of archival boxes, part 1: material and environmental assessment. *Herit. Sci.* **12**, 24 (2024).

13. Chiantore, O. & Poli, T. Indoor Air Quality in Museum Display Cases: Volatile Emissions, Materials Contributions, Impacts. *Atmosphere* **12**, 364 (2021).

14. Kearney, M., Parkin, I., Townsend, J. H., Hidalgo, M. & Curran, K. Characterisation of VOCs Surrounding Naum Gabo's Construction in Space 'Two Cones', (Tate) by in situ SPME GC-MS Monitoring. *Stud. Conserv.* **63**, 369–371 (2018).

15. Novak, M. A quantitative study of acetic acid emissions from historical cellulose acetate at room conditions. *Npj Herit. Sci* **13**, 22 (2025).

16. Fenech, A. et al. Volatile aldehydes in libraries and archives. *Atmos. Environ.* **44**, 2067–2073 (2010).

17. Menart, E., de Bruin, G. & Strlič, M. Effects of NO2 and acetic acid on the stability of historic paper. *Cellulose* **21**, 3701–3713 (2014).

18. EN 15758:2010. Conservation of cultural property. Procedures and instruments for measuring temperatures of the air and the surfaces of objects. (2010).

19. EN 16242:2012. Conservation of cultural heritage. Procedures and instruments for measuring humidity in the air and moisture exchanges between air and cultural property. (2012).

20. R Core Team. R: A Language and Environment for Statistical Computing. R Foundation for Statistical Computing. https://www.R-project.org/ (2023).

21. Janssen, H. & Roels, S. Qualitative and quantitative assessment of interior moisture buffering by enclosures. *Energy Build.* **41**, 382–394 (2009).

22. Vereecken, E. & Roels, S. Review of mould prediction models and their influence on mould risk evaluation. *Build. Environ.* **51**, 296–310 (2012).

23. ISO 2528:2017. Determination of water vapour transmission rate (WVTR) — Gravimetric (dish) method (2017).

24. Othman, S. H., Edwal, S. A. M., Risyon, N. P., Basha, R. K. & Talib, R. A. Water sorption and water permeability properties of edible film made from potato peel waste. *Food Sci. Technol.* **37**, 63–70 (2017).

25. Cappitelli, F. & Sorlini, C. From Papyrus to Compact Disc: The Microbial Deterioration of Documentary Heritage. *Crit. Rev. Microbiol.* **31**, 1–10 (2005).

26. Wang, J. et al. Moisture and Oxygen Barrier Properties of Cellulose Nanomaterial-Based Films. *ACS Sustain. Chem. Eng.* **6**, 49–70 (2018).

27. Ntelia, E. & Karapanagiotis, I. Superhydrophobic Paraloid B72. *Prog. Org. Coat.* **139**, 105224 (2020).

28. Rastogi, V. K. & Samyn, P. Bio-Based Coatings for Paper Applications. *Coatings* **5**, 887–930 (2015).

29. Herrera, M. A., Mathew, A. P. & Oksman, K. Barrier and mechanical properties of plasticized and cross-linked nanocellulose coatings for paper packaging applications. *Cellulose* **24**, 3969–3980 (2017).

30. Peuhkuri, R. H. et al. Moisture Buffering of Building Materials. Moisture Buffering of Building Materials https://www.iso.org/standard/42167.html (2005).

31. ISO 24353:2008. Hygrothermal performance of building materials and products — Determination of moisture adsorption/desorption properties in response to humidity variation. (2008).

32. JIS A 1470-1. Test method of adsorption/desorption efficiency for building materials to regulate an indoor humidity - Part 1: Response method of humidity. (2002).

33. Vereecken, E., Roels, S. & Janssen, H. In situ determination of the moisture buffer potential of room enclosures. *J Build Phys* **34**, 223–246 (2011).

34. Hens, H. Building Physics - Heat, Air and Moisture: Fundamentals and Engineering Methods with Examples and Exercises. (Ernst und Sohn, Berlin, 2007).

35. Thomson, R. Heating or Dehumidification? Maintaining Appropriate Relative Humidity Levels in Historic Buildings Containing Museum Collections. *Stud. Conserv.* **65**, P321–P326 (2020).

36. Rosina, E., Zala, M. & Ammendola, A. The moisture issue affecting the historical buildings in the Po valley: A case study approach. *J. Cult. Herit.* **60**, 78–85 (2023).

37. Leijonhufvud, G. The Indoor Climate in Skokloster Castle. https://www.academia.edu/889029/The_Indoor_Climate_in_Skokloster_Castle (2019).

Acknowledgements

Author contributions

Conceptualisation: J.M., M.S. and J.G.B.; funding acquisition: MS; investigation: J.M., I.K., M.S., J.G.B. and E.V.; methodology: J.M., M.S. and J.G.B.; project administration: MS; resources: J.M., M.S. and J.G.B.; supervision: J.M., M.S. and J.G.B.; validation: J.M.; writing-original draft: J.M.; writing-review and editing: J.M., I.K., M.S., J.G.B. and E.V.; visualisation: J.M. All authors have read and agreed to the published version of the manuscript.

Competing interests

The authors declare no competing interests.

Additional information

Supplementary information The online version contains supplementary material available at https://doi.org/10.1038/s40494-025-01958-7.

Correspondence and requests for materials should be addressed to Matija Strlič.

Reprints and permissions information is available at http://www.nature.com/reprints

Publisher's note Springer Nature remains neutral with regard to jurisdictional claims in published maps and institutional affiliations.